PAPER

Adjustable hydrazine modulation of single-wall carbon nanotube network field effect transistors from p-type to n-type

IOP Publishing Nanotechnology
Nanotechnology 27 (2016) 445203 (7pp) doi:10.1088/0957-4484/27/44/445203

Adjustable hydrazine modulation of single-wall carbon nanotube network field effect transistors from p-type to n-type

Ruixuan Dai[1], Dan Xie[1], Jianlong Xu[2], Yilin Sun[1], MengXing Sun[1], Cheng Zhang[1] and Xian Li[1]

[1] Institute of Microelectronics, Tsinghua National Laboratory for Information Science and Technology (TNList), Tsinghua University, Beijing 100084, People's Republic of China
[2] Institute of Functional Nano and Soft Materials (FUNSOM), Jiangsu Key Laboratory for Carbon-based Functional Materials and Devices, Soochow University, Suzhou, Jiangsu 215123, People's Republic of China

E-mail: xiedan@tsinghua.edu.cn

Received 15 May 2016, revised 15 August 2016
Accepted for publication 19 August 2016
Published 27 September 2016

Abstract

Single-wall carbon nanotube (SWCNT) network field effect transistors (FETs), which show decent p-type electronic properties, have been fabricated. The use of hydrazine as an aqueous solution and a strong n-type dopant for the SWCNTs is demonstrated in this paper. The electrical properties are obviously tuned by hydrazine treatment at different concentrations on the surface of the SWCNT network FETs. The transport behavior of SWCNTs can be modulated from p-type to n-type, demonstrating the controllable and adjustable doping effect of hydrazine. With a higher concentration of hydrazine, more electrons can be transferred from the hydrazine molecules to the SWCNT network films, thus resulting in a change of threshold voltage, carrier mobility and on-current. By cleaning the device, the hydrazine doping effects vanish, which indicates that the doping effects of hydrazine are reversible. Through x-ray photoelectron spectroscopy (XPS) characterization, the doping effects of hydrazine have also been studied.

Keywords: single-wall carbon nanotube, field effect transistors, hydrazine modulation, n-type, network film

(Some figures may appear in colour only in the online journal)

1. Introduction

The urge for more powerful computing ability is propelling the scaling-down of electronic devices. Low-dimensional materials can provide promising substitutions in post-silicon nanoelectronics. Being a remarkable representative of low-dimensional materials, the semiconducting single-wall carbon nanotube (SWCNT) has drawn great attention in research due to its high carrier mobility [1], high on/off ratio [2] and one-dimensional structure [3], which has great potential for scaling down. Alterable p- and n-type SWCNT doping can be employed in different fields such as light-emitting diodes, solar cells and field effect transistors (FETs) [4–6]. When applied as channels in FETs, SWCNTs can be both single- or parallel-aligned and randomly network deposited. Compared with single- or parallel-aligned SWCNT FETs, SWCNT network FETs have great advantages in fabrication. SWCNT network films can largely be synthesized and are suitable for practical integrated processes. However, SWCNTs usually exhibit p-type characteristics in the ambient environment owing to the electron withdrawing by the absorption of oxygen molecules [7]. Some research on the altering of SWCNTs so that they have n-type characteristics has been reported. Employing a special metal for the source/drain (S/D) electrodes [8] and electron-doping by surface treatment on the SWCNT surface [9] are two ways of reversing their conducting properties. Special metal contacts like yttrium (Y) and scandium (Sc) only function in single- or parallel-aligned

SWCNT FETs [8]. Electron-doping with dopants can be applied in both single- or parallel-aligned SWCNT FETs and SWCNT network FETs. This is mainly accomplished in two ways: one is to utilize alkali metal either by vaporing particles onto the SWCNT surface or by intercalating metal ions onto the SWCNT surface using aprotic solvents such as DMSO [10]. However, some treatments with alkali metals are not reversible, and can introduce immense defects to the SWCNT. These can be observed via an increased D band in the Raman spectra [11], thus degenerating conducting ability. The other is to adopt donating molecules like benzyl viologens [12], hydrazine [13] and amine-containing polymers like polyetherimide (PEI) [14].

Among all electron-donating dopants, Hydrazine is a feasible variety which has been applied in the doping of graphene and other semiconductors [15]. It has relatively intense doping effects compared to other donating molecules such as PEI [14], which cannot provide n-doping levels that are high enough for SWCNTs. Hydrazine is a small inorganic molecule with strong reducing properties, and usually serves as a donating dopant. By a simple drop-casting method, it can be used to treat SWCNTs. The doping effects of single-aligned SWCNT FETs have been reported before [16]. However, little research has concentrated on SWCNT network FETs. Therefore, there is a need to investigate hydrazine doping effects and mechanisms on SWCNT network FETs.

In this work, SWCNT network FETs which show decent p-type conducting properties are fabricated. The n-type doping effects of hydrazine on the conducting properties of different concentrations have been studied. The conversion of the conducting polarity from p-type to n-type is observed upon hydrazine surface doping, and it is found that the hydrazine doping effects are reversible. The mechanisms of hydrazine doping are also discussed.

2. Methods

2.1. Device fabrication

Heavily p-doped silicon was used as the substrate, and a 90 nm thick SiO_2 layer gate dielectric was thermally grown on it. Then the S/D electrodes were patterned using photolithography, followed by e-beam evaporation of the Cr/Au (10/50 nm) films and the lift-off process. Later, the SWCNT network film was deposited by the drop-casting method. Poly-L-lysine (0.1% w/v in water, Sigma-Aldrich) solution was first dropped onto the substrate to functionalize the surface for more adhesion. Then, rinsed by deionized (DI) water, the substrate was immersed in purified 98% semiconductor-enriched SWCNT solution (NanoIntegris, Inc.) for 1 h. After that, it was thoroughly rinsed with DI water and dried with a nitrogen gun [17]. This treatment provided the uniform assembly of the SWCNT network film over the entire surface of the substrate except the S/D area. Finally, the channel area was defined by means of photolithography and subsequently etched with O_2 plasma. Figure 1(a) demonstrates the fabricating processes of the original p-type SWCNT network FETs. Figures 1(b) and (c) show the schematic structure and the optical micrograph of the SWCNT network FET devices, respectively.

2.2. Hydrazine treatment

To investigate the doping effects of hydrazine, we prepared different concentrations (6.5 wt%, 13 wt%, 19.5 wt%, 26 wt%) of hydrazine aqueous solution by diluting a concentrated $N_2H_4 \cdot H_2O$ solution (from Sigma-Aldrich, N_2H_4 64% ~ 65%, reagent grade 98%). Figure 2 shows the hydrazine solution treatment, measuring, and cleaning procedures for the SWCNT network FETs. All the experiments were done at room temperature in ambient atmosphere. The device was first immersed in hydrazine aqueous solution for 30 min, then dried with a low mass flow nitrogen gun, as shown in figure 2(a). After the doping step, the device was measured with an Agilent B1500 semiconductor device parameter analyzer, as shown in figure 2(b). The transport and output characteristics of the SWCNT network FETs were tested with a gate voltage directly applied to the heavily p-doped Si substrate. The SWCNT network FETs were dipped into deionized (DI) water for 30 min, then rinsed with running DI water for 3 min, and dried with a high mass flow nitrogen gun for 3 min, as shown in figure 2(c). In our work, hydrazine treatment at different concentrations was performed on the same device.

3. Results and discussion

The SWCNT network films on the Si/SiO_2 substrate were characterized by atomic force microscope (AFM) and Raman spectroscopy. Figure 3(a) shows the AFM micrograph of the network structure of the SWCNT film. The maximum roughness is about 7.25 nm. The density of the carbon nanotube film is about 50 tubes μm^{-2}. In figure 3(b), Raman spectroscopy with an excitation wavelength of 514.5 nm was performed. The absence of a defect-related D band and a multi-Lorentzian G-band at 1540–1630 cm^{-1} demonstrates the high purity of the semi-conducting behavior of the SWCNT network [17]. The diameter of the SWCNTs is calculated to be 1.0 ~ 1.7 nm from the radical breathing modes (RBM), whose peak is at 176.7 cm^{-1} [18].

3.1. Electrical properties of the original p-type SWCNT network FETs

Figure 4 shows the drain current-gate voltage (I_{DS}–V_{GS}) curves and drain current-drain voltage (I_{DS}–V_{DS}) curves of one typical SWCNT network FET. The transfer characteristics in the logarithmic coordinate from 20 V to −20 V at $V_{DS} = -5$ V are shown in figure 4(a), of which the inset is in the linear coordinate. It can be seen that the original SWCNT network FETs have decent p-type conducting properties with a high on/off ratio up to 10^6, and a maximum on-current reached at about 13 μA. Figure 4(b) shows the I_{DS}–V_{DS} curves. The V_{DS} is from 0 V to −10 V, and the V_{GS} is from

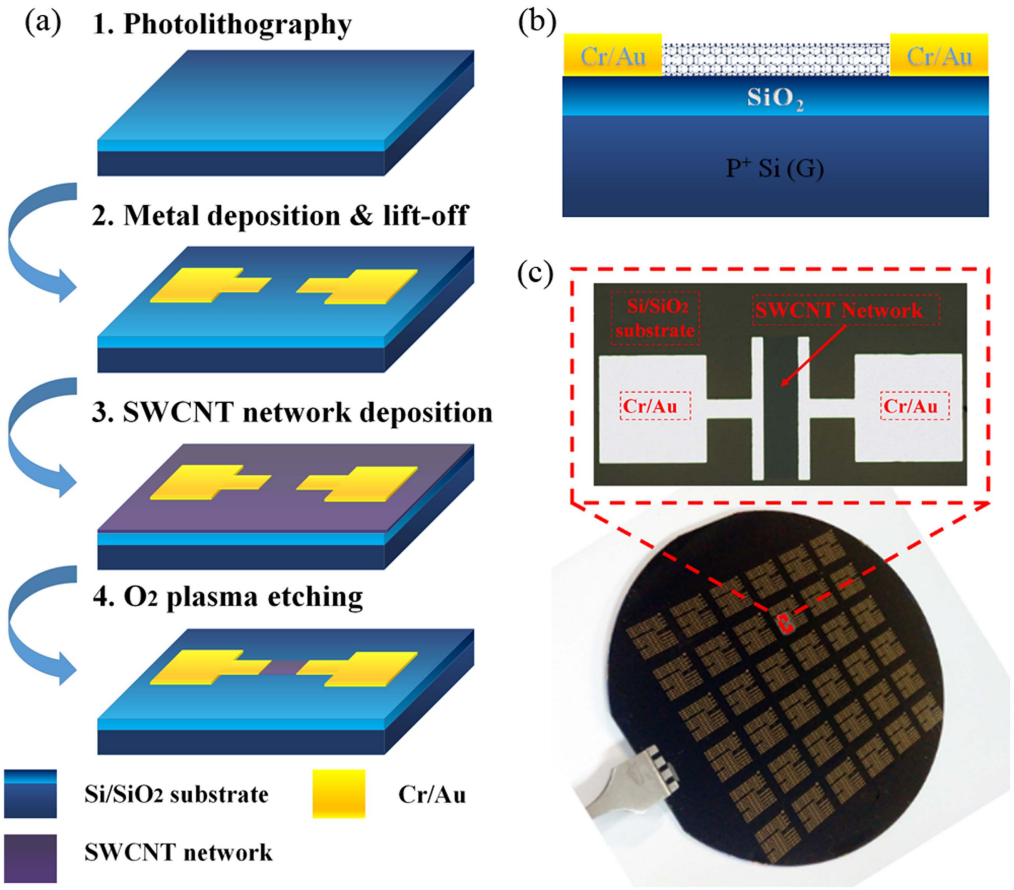

Figure 1. (a) The fabrication process of the SWCNT network FETs. (b) A schematic of one original SWCNT network FET. (c) An optical micrograph of the FET and a photograph of the whole 4-inch prepared substrate.

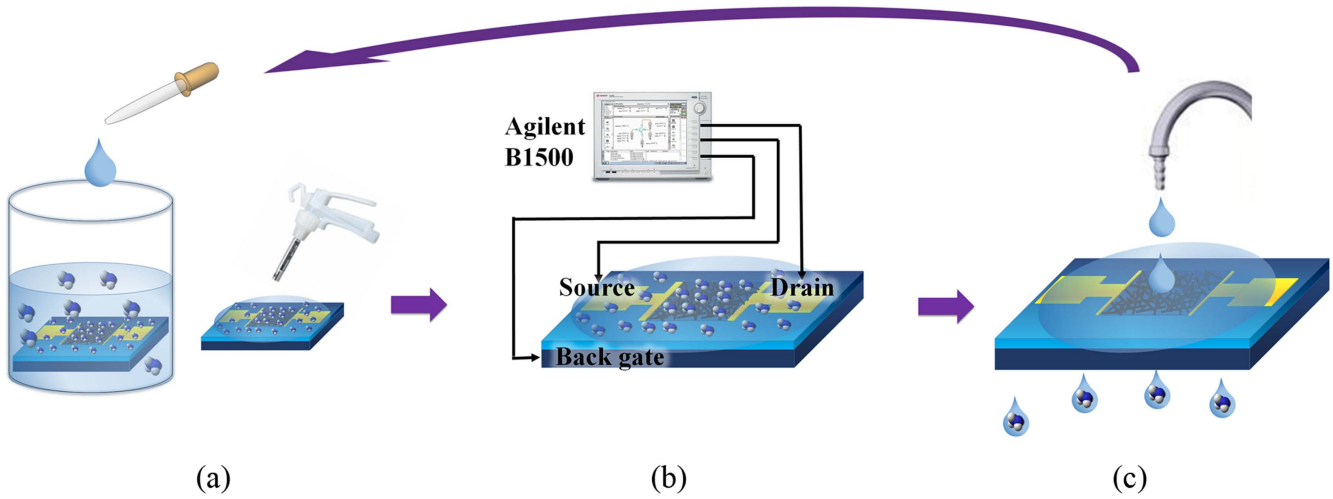

Figure 2. The hydrazine solution treatment, measuring, and cleaning procedures for the SWCNT network FETs. (a) Treatment in hydrazine aqueous solution and drying with a low mass flow nitrogen gun. (b) Measurement with the Agilent B1500. (c) Cleaning the FETs with running deionized water.

20 V to −20 V at the 4 V step. This indicates good saturation properties at $V_{DS} = -6$ V in the output curves, and the linear region shows good ohmic contacts between the SWCNTs and S/D electrodes. It is found that the output characteristic is effectively controlled by the gate. Oxygen molecules are responsible for the p-type behavior. The SWCNT network was able to absorb the oxygen molecules, making electron conductivity decrease. The holes thus become the major carriers and the SWCNT network FETs show p-type behavior [7].

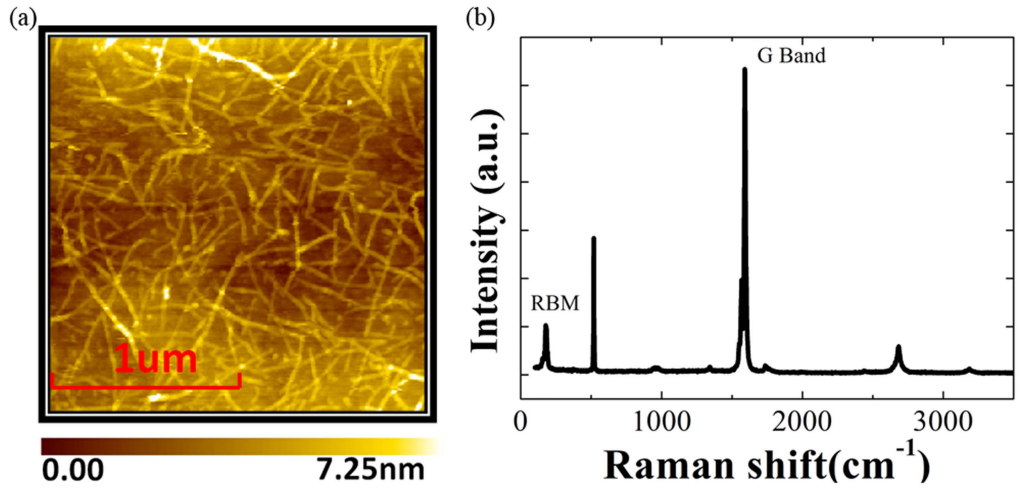

Figure 3. (a) The AFM image; (b) Raman spectroscopy of the SWCNT network film.

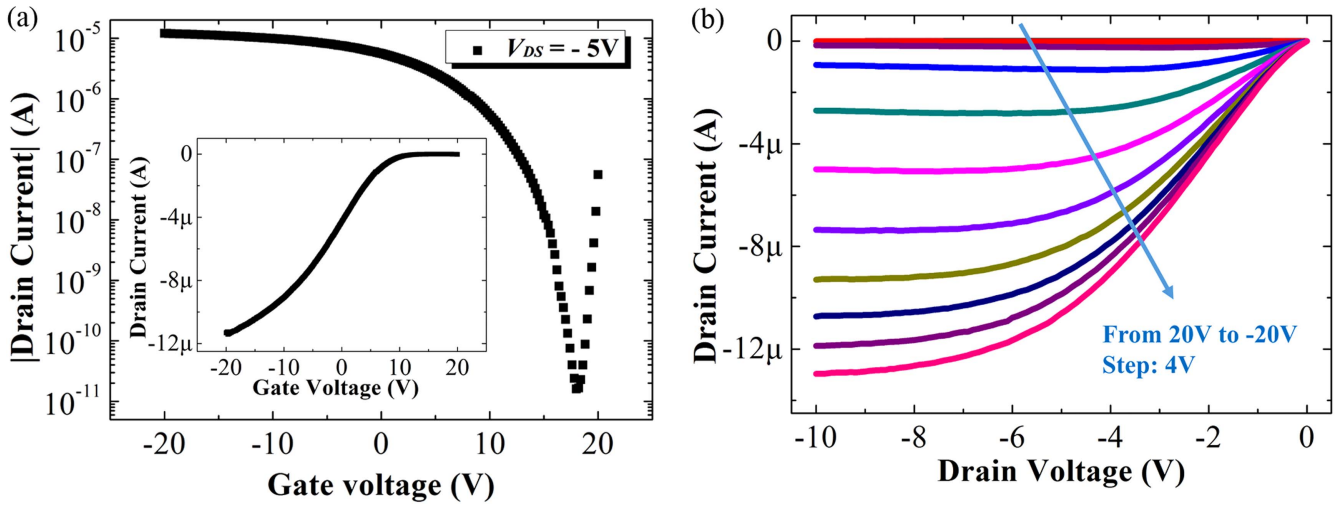

Figure 4. (a) The I_{DS}–V_{GS} curve of a typical p-type SWCNT network FET in a logarithmic coordinate with V_{GS} from 20 V to −20 V at V_{DS} = −5 V. The inset is the I_{DS}–V_{GS} curve in the linear coordinate. (b) The I_{DS}–V_{DS} curves of the same FET sample with V_{DS} from 0 V to −10 V and the V_{GS} from 20 V to −20 V at the 4 V step.

3.2. Hydrazine modulation on the electrical characteristics of SWCNT network FETs

Figure 5(a) demonstrates the logarithmic I_{DS}–V_{GS} curves of the SWCNT network FETs after being treated with hydrazine at different concentrations, and the inset shows the I_{DS}–V_{GS} curves in the linear coordinate with V_{GS} from −20 V to 20 V at V_{DS} = 5 V. It is found that the transfer characteristics of SWCNT network FETs greatly depend on the concentration of the hydrazine. When treated with a hydrazine concentration of 6.5%, the SWCNT network FETs show a bipolar shape. The aqueous solution with 6.5% hydrazine can provide some n-type doping effects, but p-type behavior still exists. The current at V_{GS} = −20 V is still very high compared with that at V_{GS} = 20 V. At a 13% hydrazine concentration, the current at V_{GS} = −20 V is relatively low. The p-type behavior almost disappears and the FETs show n-type behavior. At a higher concentration of hydrazine, the n-type conducting properties become stronger and the p-type devices are totally transferred to the n-type devices. At concentrations higher than 26%, the devices deteriorated with the off-current increasing dramatically. Therefore, the SWCNT FETs treated with the hydrazine aqueous solution at increasing concentrations switch from unipolar p-type to ambipolar, and finally to n-type behavior. Figure 5(b) is one of the representative output curves for a hydrazine concentration of 19.5%. The output characteristic curves display saturation at V_{DS} = 5 V, and the linear region indicates good ohmic contacts between the SWCNTs and source/drain electrodes. The output characteristic curves of other hydrazine concentrations have a similar appearance with the 19.5% concentration.

To characterize the influence of different hydrazine concentrations on the doping effect in detail, several of the electrical parameters of the SWCNT network FETs treated with hydrazine have been extracted. Figure 5(c) shows the on-current comparison of the SWCNT network FETs before (V_{GS} = −20 V) and after hydrazine treatment (V_{GS} = 20 V). The red line is nearly horizontal, showing that the devices

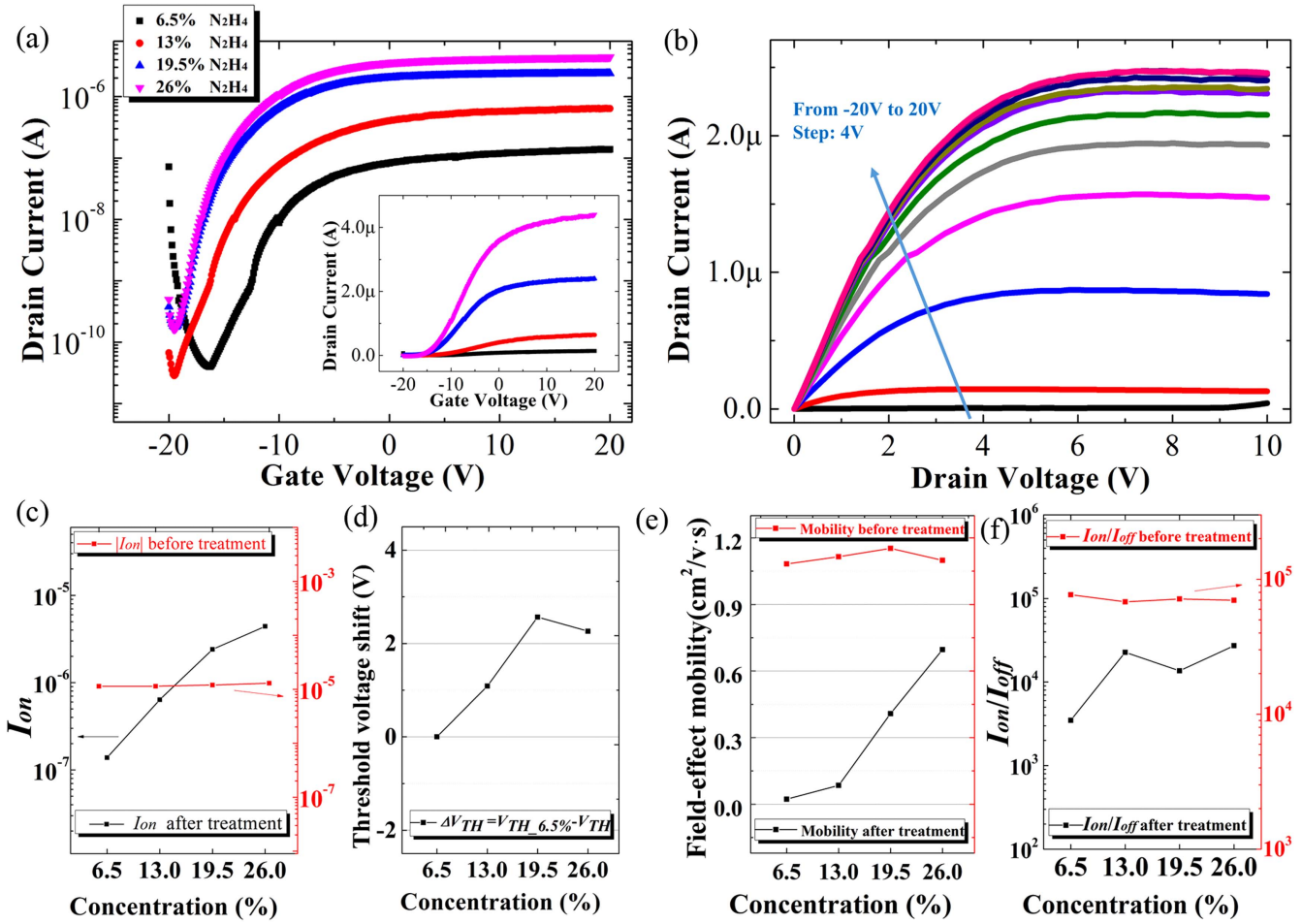

Figure 5. (a) The I_{DS}–V_{DS} curves of different hydrazine-treated SWCNT network FETs in the logarithmic coordinate, with V_{GS} from −20 V to 20 V at V_{DS} = 5 V. The inset shows the I_{DS}–V_{DS} curves in the linear coordinate. (b) The I_{DS}–V_{DS} curves of the 19.5% hydrazine-treated SWCNT network FETs with V_{DS} from 0 V to 10 V and the V_{GS} from −20 V to 20 V at the 4 V step. (c) The on-current curve of the original SWCNT network FETs (red dots and line) and after treatment with hydrazine (black dots and line). (d) A plot of the threshold voltage shift versus hydrazine concentration. (e) A plot of field-effect mobility versus hydrazine concentration. The black dots and line represent this after treatment, and the reds dot and line represent it before. (f) A plot of the on/off ratio versus hydrazine concentration. The black dots and line represent this after treatment, and the red dots and line represent it before.

keep the same p-type behavior each time before the hydrazine treatment process. Through the cleaning method mentioned above, the original p-type state of the hydrazine-treated SWCNT network FETs can be reversed, demonstrating that the hydrazine treating effects are reversible. The black line has an obvious ascending trend, which indicates that with a higher concentration of hydrazine, there would be an increasing amount of electron carriers, thus improving the on-current of the SWCNT network FETs. Figure 5(d) shows the plot of the threshold voltage shift versus hydrazine concentration. The threshold voltage shift at 6.5% hydrazine is defined as zero, and the shift of other concentrations (ΔV_{TH}) is obtained by the formula: $\Delta V_{TH} = V_{TH\_6.5\%} - V_{TH}$. In the equation, $V_{TH\_6.5\%}$ is the threshold voltage at 6.5% hydrazine and V_{TH} is the threshold voltage at other concentrations. The threshold voltages were extracted by extrapolation of the linear region method [19]. There is an obviously ascending trend before the 19.5% hydrazine concentration; after this, the shift decreases. The relation of field-effect mobility versus hydrazine concentration is displayed in figure 5(e). The mobility of SWCNT network FETs is calculated by the following equations:

$$\mu = \frac{g_m \cdot l}{C_g \cdot V_{DS} \cdot W} \quad (1)$$

$$C_g = \frac{\varepsilon_{ox}}{t_{ox}} \quad (2)$$

where g_m is the maximum of transconductance in the transfer characteristic, l is the length of the device, w is the width, V_{DS} is the drain voltage, C_g is the capacitance of the SiO_2 dielectric layer, ε_{ox} is the dielectric constant of SiO_2 and the t_{ox} is the thickness. A notable rise in mobility with an increasing concentration of hydrazine can be found in the hydrazine-treated devices. This phenomenon may be attributed to the fact that increasing the concentration of hydrazine provides more electrons in the channel [20]. The mobility before hydrazine treatment is about 1.1 $cm^2\ v^{-1} \cdot s$, shown with red dots, and hole mobility can also recover to be at almost the same level after hydrazine removal. Figure 5(f) shows the curve for on/off ratio versus hydrazine concentration; no

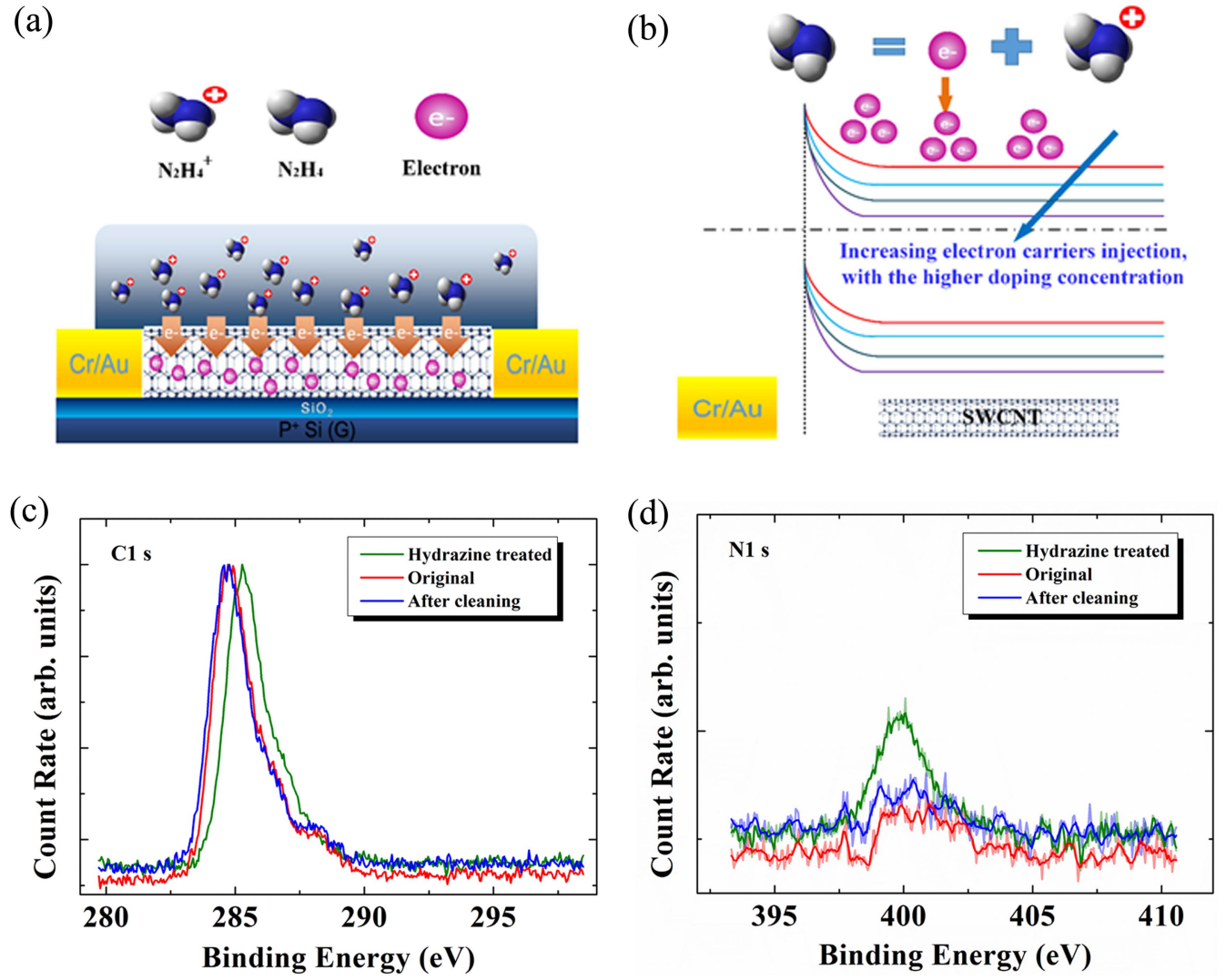

Figure 6. (a) A schematic diagram of the doping process on the SWCNT network FETs. (b) A schematic diagram of the Fermi level shifts. The XPS spectra of (c) C 1 s (normalized) and (d) N 1 s (normalized to the C 1 s peak) for the SWCNT network film before and after 19.5% hydrazine treatment, as well as the film after cleaning.

obvious change in the on/off ratio can be observed, with the hydrazine doping concentration increasing and remaining at about 10^4, showing its potential for application in complementary circuit design.

3.3. Mechanism of hydrazine doping on SWCNT network FETs

Concluded from the distinct doping effects demonstrated above, hydrazine is an effective dopant for SWCNTs. The mechanism of this hydrazine doping effect could be a result of the charge transferring from the hydrazine molecules to the SWCNTs. Hydrazine is a strong reductant, which can easily provide an electron for SWCNTs. The SWCNTs obtain electrons from the hydrazine molecules over the SWCNT network film, and one hydrazine molecule donates an electron to form $N_2H_4^+$ [16]. No strong chemical bond can exist between the SWCNT and hydrazine; thus, they may be bonded by van der Waals forces. So, hydrazine molecules can be removed by DI water. Figure 6(a) shows a schematic diagram of the doping process. As for original SWCNTs, holes are the majority of the carriers, and the Fermi level is close to the valence band displaying p-type behavior. After hydrazine treatment, the holes become the minority of the carriers, and the electrons increase in the SWCNTs, bringing the Fermi level close to the conduction band [16]. So, when the gate voltage is less than the threshold voltage, there are little holes contributing to the current, keeping the off-current low. After a voltage higher than the threshold voltage is applied to the gate, more electrons transfer into the SWCNTs, turning the channel into an on-state. The electrons become the majority of the carriers, showing n-type behavior. Besides this, with an increasing concentration of hydrazine, the density of the electrons increases, and the SWCNT obtains an increasing number of electrons from the hydrazine molecules at the same gate voltage. Therefore, the Fermi level shifts closer to the conduction band, as shown in figure 6(b).

To further investigate the doping effect and the mechanism of hydrazine, we performed x-ray photoelectron

spectroscopy (XPS). For XPS to probe the binding energy of core electrons, it is sensitive to changes in the Fermi level. Doping with hydrazine would result in a charge transfer from hydrazine molecules to the SWCNTs, so Fermi level shifts due to the charge transfer will be reflected by the binding energy shifts of the C 1 s peak. An upshift of the Fermi level will incur a shift towards a higher binding energy, and vice versa. According to previous research on the XPS of SWCNT, p-doped SWCNTs with a C1 s peak shift toward a lower binding energy, and the n-doped SWCNTs expect an upshift in the C1 s peak [21, 22]. Figure 6(c) displays the core-level XPS spectrum (normalized) for the original SWCNT network film before and after 19.5% hydrazine treatment, and the film after cleaning. There are notable C 1 s peak up-shifts at about 0.4 eV between the original and hydrazine-treated film, which reveal the upshift of the Fermi level after hydrazine treatment. The hydrazine molecules inject ample electrons into the SWCNT network film, raising the Fermi level to the conduction band, indicating n-type behavior. Besides this, we also noticed that after cleaning, the doping shift vanishes. Figure 6(d) shows the N 1 s spectra of the XPS (normalized to the C 1 s peak). It can be seen that there is no obvious peak of N 1 s in the original film before hydrazine treatment. However, after hydrazine treatment, a distinct N 1 s peak appears around 400 eV, which suggests that after treatment, the hydrazine molecules stay on the SWCNT network surface. In addition, the N 1 s peak almost disappears after the film had been cleaned, once again demonstrating that the doping effect is due to the charge transferring, that there can be no strong chemical bonds between the hydrazine and SWCNT, and that the doping processes are reversible.

4. Conclusions

In this paper, SWCNT network FETs have been fabricated and the hydrazine doping effects involving the concentration and the doping mechanism investigated. It is found that hydrazine molecules are effective electron dopants, which can provide enough electrons to turn p-type SWCNT network FETs into n-type ones. The hydrazine exhibits distinct electron-doping effects on the SWCNT network FETs and such effects are reversible. Besides this, the doping effects of hydrazine greatly depend on concentration, and a higher concentration of hydrazine can supply stronger doping effects. The on-current and mobility of the n-type SWCNT FET increases with an increase in hydrazine concentration. The threshold voltage also shows a dependence on the concentration and its shift increases before a 19.5% concentration of hydrazine is reached. The on/off ratio of n-type SWCNT network FETs does not deteriorate with concentration increase, and remains about 10^4. This is important for the potential applications of SWCNT network FETs in complementary logic circuits.

Acknowledgments

The authors are grateful for the financial support from the National Natural Science Foundation of China (51372130 and 51372133), and the Tsinghua National Laboratory for Information Science and Technology (TNList) Cross-discipline Foundation.

References

[1] Snow E S, Campbell P M, Ancona M G and Novak J P 2005 *Appl. Phys. Lett.* **17** 033105
[2] Kang S J, Kocabas C, Ozel T, Shim M, Pimparkar N, Alam M A, Rotkin S V and Rogers J A 2007 *Nat. Nanotechnol.* **2** 230–6
[3] Iijima S 1991 Helical *Nature* **354** 56–8
[4] Tenent R C, Barnes T M, Bergeson J D, Ferguson A J, To B, Gedvilas L M, Heben M J and Blackburn J L 2009 *Adv. Mater.* **21** 3210–6
[5] Ou E C *et al* 2009 *ACS Nano* **3** 2258–64
[6] Rowell M W, Topinka M A, McGehee M D, Prall H J, Dennler G, Sariciftci N S, Hu L and Gruner G 2006 *Appl. Phys. Lett.* **88** 233506
[7] Kang D, Park N, Ko J H, Bae E and Park W 2005 *Nanotechnology* **16** 1048
[8] Ding L *et al* 2009 *Nano Lett.* **9** 4209–14
[9] Wang H *et al* 2014 *Proc. Natl Acad. Sci.* **111** 4776–81
[10] Pénicaud A, Poulin P, Derré A, Anglaret E and Petit P 2005 *JACS* **127** 8–9
[11] Claye A, Rahman S, Fischer J E, Sirenko A, Sumanasekera G U and Eklund P C 2001 *Chem. Phys. Lett.* **333** 16–22
[12] Kim S M *et al* 2008 *JACS* **131** 327–31
[13] Feng T, Xie D, Wang D, Wen L and Wu M 2014 *J. Appl. Phys.* **116** 224511
[14] Feng T, Xie D, Zhao H, Li G, Xu J, Ren T and Zhu H 2013 *Appl. Phys. Lett.* **103** 193502
[15] Talapin D V and Murray C B 2005 *Science* **310** 86–9
[16] Klinke C, Chen J, Afzali A and Avouris P 2005 *Nano Lett.* **5** 555–8
[17] Ha T J, Chen K, Chuang S, Yu K M, Kiriya D and Javey A 2014 *Nano Lett.* **15** 392–7
[18] Jorio A, Pimenta M A, Souza Filho A G, Saito R, Dresselhaus G and Dresselhaus M S 2003 *New J. Phys.* **5** 139
[19] Ortiz-Conde A, Sánchez F G, Liou J J, Cerdeira A, Estrada M and Yue Y 2002 *Microelectron. Reliab.* **42** 583–96
[20] Shuttle C G, Hamilton R, Nelson J, O'Regan B C and Durrant J R 2010 *Adv. Funct. Mater.* **20** 698–702
[21] Mistry K S, Larsen B A, Bergeson J D, Barnes T M, Teeter G, Engtrakul C and Blackburn J L 2011 *ACS Nano* **5** 3714–23
[22] Graupner R, Abraham J, Vencelová A, Seyller T, Hennrich F, Kappes M M, Hirsch A and Ley L 2003 *Phys. Chem. Chem. Phys.* **5** 5472–6